The Plant Cell, Vol. 20: 2497–2513, September 2008, www.plantcell.org

Transport and Sorting of the *Solanum tuberosum* Sucrose Transporter SUT1 Is Affected by Posttranslational Modification [W]

Undine Krügel,[a] Liesbeth M. Veenhoff,[b] Jennifer Langbein,[c] Elena Wiederhold,[b] Johannes Liesche,[a] Thomas Friedrich,[c] Bernhard Grimm,[a] Enrico Martinoia,[d] Bert Poolman,[b] and Christina Kühn[a,1]

[a] Institute of Biology, Department of Plant Physiology, Humboldt University, 10115 Berlin, Germany
[b] Department of Biochemistry, Groningen Biomolecular Sciences and Biotechnology Institute, Zernike Institute for Advanced Materials, University of Groningen, 9747 AG, Groningen, The Netherlands
[c] Institute of Chemistry, Technical University of Berlin, 10623 Berlin, Germany
[d] Institute of Plant Biology, University of Zürich, CH-8008 Zurich, Switzerland

The plant sucrose transporter SUT1 from *Solanum tuberosum* revealed a dramatic redox-dependent increase in sucrose transport activity when heterologously expressed in *Saccharomyces cerevisiae*. Plant plasma membrane vesicles do not show any change in proton flux across the plasma membrane in the presence of redox reagents, indicating a SUT1-specific effect of redox reagents. Redox-dependent sucrose transport activity was confirmed electrophysiologically in *Xenopus laevis* oocytes with SUT1 from maize (*Zea mays*). Localization studies of green fluorescent protein fusion constructs showed that an oxidative environment increased the targeting of SUT1 to the plasma membrane where the protein concentrates in 200- to 300-nm raft-like microdomains. Using plant plasma membranes, St SUT1 can be detected in the detergent-resistant membrane fraction. Importantly, in yeast and in plants, oxidative reagents induced a shift in the monomer to dimer equilibrium of the St SUT1 protein and increased the fraction of dimer. Biochemical methods confirmed the capacity of SUT1 to form a dimer in plants and yeast cells in a redox-dependent manner. Blue native PAGE, chemical cross-linking, and immunoprecipitation, as well as the analysis of transgenic plants with reduced expression of St SUT1, confirmed the dimerization of St SUT1 and Sl SUT1 (from *Solanum lycopersicum*) in planta. The ability to form homodimers in plant cells was analyzed by the split yellow fluorescent protein technique in transiently transformed tobacco (*Nicotiana tabacum*) leaves and protoplasts. Oligomerization seems to be cell type specific since under native-like conditions, a phloem-specific reduction of the dimeric form of the St SUT1 protein was detectable in SUT1 antisense plants, whereas constitutively inhibited antisense plants showed reduction only of the monomeric form. The role of redox control of sucrose transport in plants is discussed.

INTRODUCTION

It has previously been reported that sucrose transporter function is severely affected by thiol group modifying agents (Lichtner and Spanswick, 1981; Bourquin et al., 1990). Sucrose uptake in soybean (*Glycine max*) cotyledons is sensitive to the sulfhydryl-modifying compounds *N*-ethylmaleimide (NEM) and *p*-chloromercuribenzenesulfonate (pCMBS), and the thiol-reducing agent DTE fully reverses the pCMBS inhibition but not that of NEM (Lichtner and Spanswick, 1981). Measurements using *Vicia faba* leaf discs revealed that treatment with Cys or dithioerythreitol reversed inhibition by pCMBS pretreatment (M'Batchi and Delrot, 1984). Observations with plasma membrane vesicles (PMVs) from sugar beet (*Beta vulgaris*) showed that diethylpyrocarbonate binding was substrate protectable, whereas pCMBS activity was not linked to substrate binding (Bush, 1989, 1993).

It was also shown that sodium sulfite (SO_2) affects sucrose uptake in PMVs of *Vicia faba* without affecting the two components of the proton motive force, the delta pH, and the membrane potential $\Delta\Psi$. Moreover, sulfite did not inhibit the H^+-pumping ATPase of the PMVs, suggesting a direct inhibition of the sucrose carrier (Maurousset et al., 1992).

Yeast cells transformed with a plasmid expressing the sucrose transporter So SUT1 from spinach (*Spinacia oleracea*) showed a pH-dependent uptake of sucrose with a K_m of 1.5 mM, which could be inhibited by maltose, α-phenylglucoside, carbonyl cyanide *m*-chlorophenylhydrazone, and pCMBS (Riesmeier et al., 1992). Similar transport characteristics are described for the potato (*Solanum tuberosum*) sucrose transporter SUT1 with a K_m of 1 mM (Riesmeier et al., 1993; Boorer et al., 1996). St SUT1 is the main sucrose transporter in potato plants responsible for phloem loading, as demonstrated in transgenic plants with lowered St SUT1 levels (Riesmeier et al., 1994; Kühn et al., 1996). St SUT1 belongs to the major facilitator superfamily and transduces free energy from the proton motive force into a

[1] Address correspondence to christina.kuehn@biologie.hu-berlin.de.
The author responsible for distribution of materials integral to the findings presented in this article in accordance with the policy described in the Instructions for Authors (www.plantcell.org) is: Christina Kühn (christina.kuehn@biologie.hu-berlin.de).
[W] Online version contains Web-only data.
www.plantcell.org/cgi/doi/10.1105/tpc.108.058271

substrate concentration gradient by transporting sucrose in symport with a proton (Boorer et al., 1996).

Protein–protein interactions play an important role in the function and regulation of proteins in general. The function of many bacterial and mammalian membrane transport proteins is coupled to their oligomeric state (reviewed in Veenhoff et al., 2002). Preliminary evidence for oligomerization of sucrose transporter proteins from tomato (*Solanum lycopersicum*) has been obtained using the yeast two-hybrid split-ubiquitin system (Reinders et al., 2002).

Our aim is to elucidate the effect of redox reagents on the specific activity of plant sucrose transporters. Here, we report on the reversible regulation of the SUT1 transport activity in plant and yeast using a variety of biochemical methods. We employed transport and targeting assays, blue native PAGE (BN-PAGE), chemical cross-linking, immunoprecipitation, bimolecular fluorescence complementation (BiFC), immunolocalization and the analysis of transgenic plants with reduced expression of St *SUT1* to probe the structure and function of the protein. We show that oxidation of the St SUT1 protein drastically increases its activity and affects its targeting in yeast. The increase in activity and the plasma membrane targeting are paralleled by a change in the oligomeric state of the transporter. Interestingly, plasma membrane targeting of the transporter in yeast is more efficient in the presence of oxidizing agents, and the protein becomes concentrated in 200-nm lipid raft-like microdomains. St SUT1 was detected in the detergent-resistant membrane (DRM) fraction from plants, and whether SUT1 is raft associated in plants is discussed.

RESULTS

Oxidizing Agents Increase the Rates of Sucrose Uptake in Yeast

To analyze the impact of redox reagents in the sucrose transport activity of St SUT1, we performed sucrose uptake experiments in yeast in the presence or absence of reducing or oxidizing agents. In the presence of reducing agents such as DTT or reduced GSH, the SUT1 uptake characteristics are decreased by 50% or even more compared with the untreated transporter (Figure 1A). The opposite effect can be observed upon oxidation of the transporter. After only 5 min of preincubation of yeast cells with L-cystine, the rate of uptake was ~10-fold higher than after preincubation with Cys (Figure 1B). Oxidized glutathione (GSSG) had an even more pronounced stimulating effect (Figure 1C). Application of protonophores, like CCCP, resulted in the complete loss of sucrose uptake even in the presence of 10 mM oxidized glutathione (Figure 1C), indicating that sucrose transport catalyzed by the oxidized SUT1 is still proton coupled as previously shown for the reduced form of the transporter (Boorer et al., 1996).

This redox-dependent inhibition of the SUT1 activity is reversible, since the inhibitory effect of DTT at 10 mM can be reversed by application of only 5 mM of GSSG (Figure 1D). The $K_{0.5}$ of GSSG was determined by testing different concentrations of glutathione (1, 5, 10, 20, and 50 mM oxidized glutathione). The $K_{0.5}$ value of oxidized glutathione GSSG was determined to be 3 mM in the presence of 1 mM sucrose (Figure 1E). The optimal DTT-to-GSSG ratio was determined in yeast (Figure 1F), and sucrose uptake was optimal at 9 mM GSSG to 1 mM DTT, indicating that the presence of an electron donor is required for optimal redox activation.

Determination of the K_m and V_{max} of SUT1 under oxidizing conditions revealed that the K_m was 1 mM, which corresponds to the value reported by our group for this transporter and published data of SUT1 homologs (Riesmeier et al., 1993). By contrast, the V_{max} was increased by a factor of ~10 compared with the values reported and measured in our laboratory (Figure 1G; Boorer et al., 1996).

Redox Control Affects Targeting and Function in Yeast

The prominent increase in SUT1-mediated sucrose uptake in yeast upon application of oxidizing agents might be caused by conformational changes of the protein and by inter- and/or intramolecular disulfide formation, but in part also by differences in localization. To test the hypothesis that efficient targeting of the SUT1 protein to the plasma membrane was affected by the redox state of the environment, we analyzed a functional Sl SUT1–green fluorescent protein (GFP) fusion (Reinders et al., 2002) in yeast in the presence or absence of reducing or oxidizing agents. Sl SUT1-GFP was previously shown to be functional in sucrose uptake and is able to complement a sucrose uptake-deficient yeast mutant (Reinders et al., 2002; Lalonde et al., 2003). Yeast cells expressing Sl SUT1-GFP yielded GFP fluorescence at the plasma membrane and in intracellular perinuclear, most likely endoplasmic reticulum (ER)–derived, membranes (Kühn, 2003). Up to 60% of the total fluorescence was retained intracellularly in endomembranes (as determined with LCS software; Leica). Staining with 4',6-diamidino-2-phenylindole confirmed the perinuclear localization (Kühn, 2003). In the presence of H_2O_2, L-cystine, or GSSG, most of the intracellular GFP fluorescence disappeared within 30 min (only 20% of the total fluorescence remained intracellularly), and GFP became distributed nonhomogenously in concentrated spots at the surface of the cell (Figures 2B, 2D, and 2F). As a control, localization under reducing conditions using DTT, GSH, or Cys showed homogenous distribution of Sl SUT1-GFP at the yeast plasma membrane and, in addition, GFP fluorescence in intracellular compartments (Figures 2A, 2C, and 2E). Similar microdomains in the plasma membrane that appeared upon oxidation have previously been described for other plant membrane proteins and endogenous transporters expressed in yeast (Grossmann et al., 2006, 2007). The diameter of Sl SUT1-GFP microdomains was estimated to be 200 to 300 nm. The sucrose uptake mediated by the Sl SUT1-GFP fusion protein in the presence of GSSG is also inducible by application of oxidizing agents as shown for the St SUT1 protein without GFP (Figure 1H).

As previously suggested for the hexose transporter *HUP1* from *Chlorella kessleri* (Grossmann et al., 2006), SUT1 activity may have been affected by its concentration in raft-like compartments and the accompanying specific lipid environment. To confirm this hypothesis, a yeast mutant deficient in ergosterol biosynthesis, *erg6*, was used for transformation with the Sl

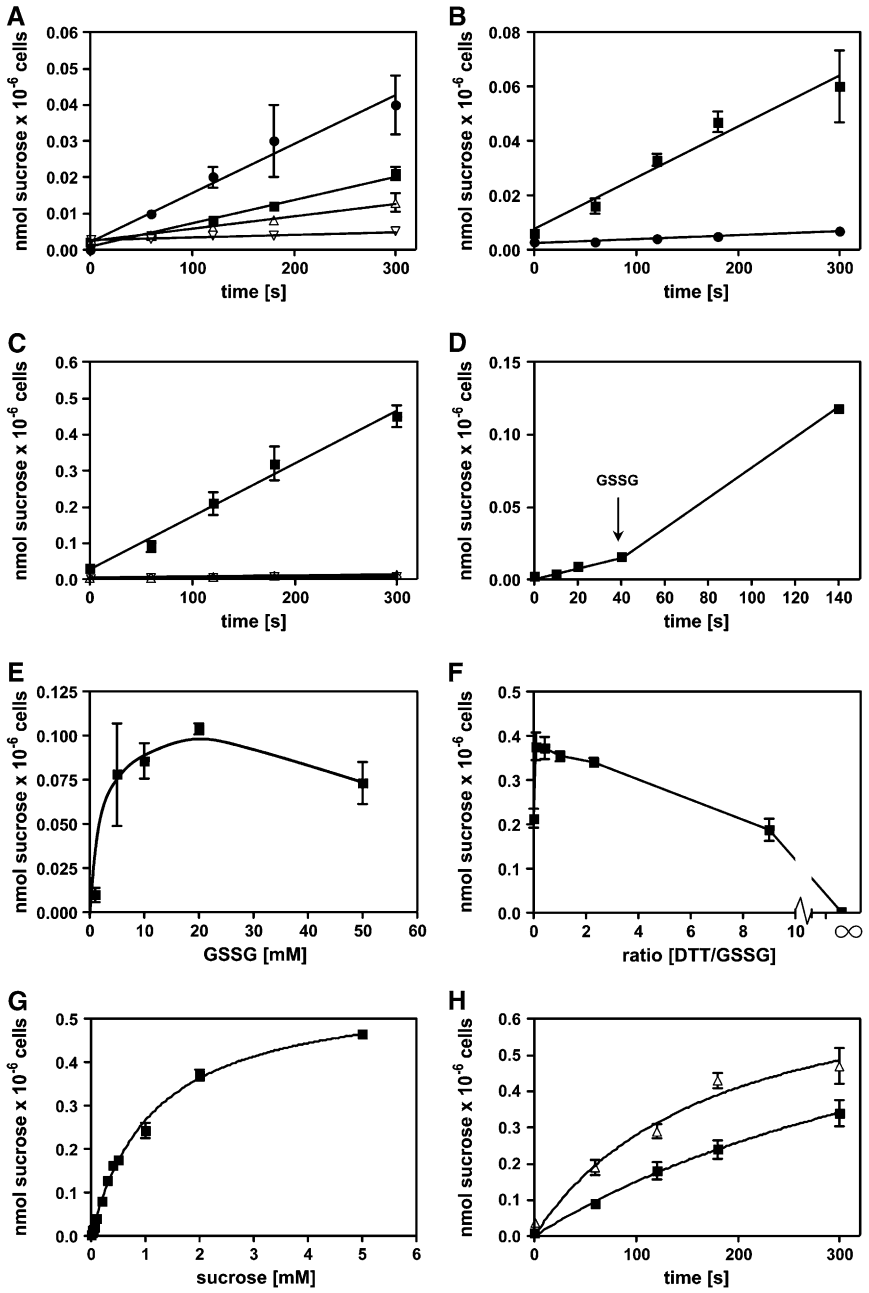

Figure 1. Analysis of St SUT1 Activity in Yeast St SUT1–Mediated ^{14}C-Sucrose Uptake into Yeast Strain SUSY7.

(A) Uptake in the presence of 10 mM DTT (squares) or 10 mM GSH (triangles) compared with the empty vector control (inverse triangles) and to the untreated control (circles). Reducing conditions slightly inhibit sucrose uptake mediated by SUT1.

(B) Uptake in the presence of 5 mM L-cystine (squares) or 5 mM Cys (circles). Samples were taken 1, 2, 3, and 5 min after addition of ^{14}C-sucrose.

(C) Uptake after 5 min of preincubation with 10 mM reduced (triangles) or oxidized glutathione (GSSG; squares). Uptake measured with the empty vector pDR195 in SUSY7 (inverse triangles) or after addition of 10 μM CCCP (circles) is indicated. Triangles, inverse triangles, and circles are overlapping.

(D) Inhibition of the St SUT1–mediated ^{14}C-sucrose uptake by 5 mM DTT is reversible by application of 5 mM GSSG after 40 s (arrow).

(E) Determination of the $K_{0.5}$ of GSSG. ^{14}C-sucrose uptake after 5 min of preincubation with different concentrations of glutathione is shown. Cells were energized by addition of glucose in a final concentration of 10 mM 1 min before uptake experiments. Uptake experiments were performed in 25 mM Na-phosphate, pH 5.4. The $K_{0.5}$ of GSSG was calculated to be 3 mM.

(F) Determination of the optimal DTT-to-GSSG ratio for uptake. Experiments were performed in the presence of 10 mM DTT or GSSG, or both in a ratio of 9:1 mM, 7:3 mM, 5:5 mM, 3:7 mM, and 1:9 mM GSSG:DTT.

SUT1-GFP fusion construct. It was previously shown for other raft-associated proteins like the hexose transporter *HUP1* that they are not concentrated in raft-like microdomains if expressed in the *erg6* mutant (Grossmann et al., 2006). Sl SUT1-GFP is also no longer associated with raft-like structures in the *erg6* mutant, even in the presence of 10 mM H_2O_2 (Figures 3A and 3B). However, the amount of intracellular GFP fluorescence is decreased in the *erg6* mutant as observed before in the yeast mutant SUSY7 if cells are treated with oxidizing agents (Figure 3B). Thus, plasma membrane (PM) targeting of the GFP fusion protein is unaffected in the *erg6* mutant, whereas organization in raft-like compartments is disturbed. Methyl-β-cyclodextrin, which is known to inhibit raft formation by cholesterol depletion, was shown to destroy H_2O_2-induced raft localization of Sl SUT1-GFP (see Supplemental Figure 1 online). A homogenous distribution of Sl SUT1-GFP at the yeast PM was observed.

Whereas in plants the nature and function of lipid raft-like structures are not very well investigated, the function of rafts in the mammalian system is related to signaling and oligomerization, and the raft-dependent endocytosis of membrane proteins is well documented (Ikonen, 2001; Parton and Richards, 2003; Laude and Prior, 2004; Hanzal-Bayer and Hancock, 2007; Lajoie and Nabi, 2007). To test whether lipid raft localization of SUT1 is related to endocytic events, yeast cells expressing a Sl SUT1-GFP fusion construct were exposed to brefeldin A, which is known to prevent exocytosis and to induce endocytic events (Samaj et al., 2004; Murphy et al., 2005). Indeed brefeldin A induces vesicle formation in the yeast strain SUSY7, which is able to form raft-like structures (Figure 3C).

The Oligomeric State of St SUT1 Expressed in Yeast

For many integral PM proteins, it has been reported that dimerization or tetramerization is a prerequisite for their efficient ER export and/or that PM targeting depends on their oligomeric state (Mikosch et al., 2006; Maurel, 2007). Two-hybrid studies in yeast revealed the capacity of Sl SUT1 to form homo- and heteromers (Reinders et al., 2002). To test whether raft association and PM targeting of the sucrose transporter is related to its oligomeric form, we performed BN-PAGE with yeast cells treated as described before for uptake measurements.

Yeast cells expressing St SUT1 were pretreated exactly as done in prior uptake measurements. The microsomal fraction of yeast cells was separated by SDS-PAGE. When reducing agents were omitted during isolation and purification, an additional protein band of high molecular mass was detectable after immunodetection with St SUT1–specific antibodies. It is proposed that this protein band represents the dimeric form of SUT1 (Figure 3D). A strong increase of this additional higher molecular mass band is observed when yeast cells have been pretreated with H_2O_2 or GSSG and equal amounts of total protein are loaded on SDS-PAGE (Figure 3D).

The fraction of dimeric St SUT1 was observed only when reducing agents were absent during the PM extraction and protein purification steps. These experiments indicate that homodimerization of St SUT1 occurred likely without additional plant-specific factors and that one or more intermolecular disulfide bonds in SUT1 could be readily formed in the heterologous expression system.

The Proton Flux across the Plant PM Is Not Affected by Redox Reagents

Sucrose-proton cotransport across the PM is driven by the proton motive force (*pmf*), which is defined by the membrane potential and the proton gradient and thus by the activity of proton-pumping PM ATPases. To exclude that the stimulating effect on the sucrose transporter activity is due to enhanced proton flux across the membrane mediated by H^+-ATPases or other proton pumping activities, we measured the total proton flux across the plant PM in response to various redox reagents via acridine orange quenching (Figure 4A). No increase in proton flux over the plant PM was observed. Thus, we can exclude that increased St SUT1 activity by oxidizing agents might be due to secondary effects on the proton gradient.

Increased Sucrose Transport Activity Is Observed Even at Constant Membrane Potential

It is already known and described in the literature that both GSH and GSSG affect the membrane potential, not only in the animal system but also in plant cells like broad bean protoplasts, and that uptake of GSH and GSSG induce ion movements over the PM (Jamai et al., 1996). A depolarization of the PM potential of broad bean mesophyll protoplasts can be observed upon GSH or GSSG uptake. To exclude that the strong effect of GSSG on sucrose transport activity might be due to secondary effects on the proton motive force, it is therefore not sufficient to analyze the effect of redox reagents on the ΔpH as done in Figure 4A, but also to analyze sucrose uptake activity at constant membrane potential. The most reliable method is therefore electrophysiological voltage-clamp experiments with constant holding potential. Since the sucrose-induced currents mediated by

Figure 1. (continued).

(G) Determination of the K_m value of SUT1 after induction with 5 mM GSSG. The K_m was unaffected upon activation with 3 mM GSSG, whereas the V_{max} increases at least 10-fold.

(H) ^{14}C-sucrose uptake into yeast strain SUSY7 catalyzed by St SUT1 (triangles) and Sl SUT1-GFP (squares) in the presence of 10 mM GSSG. The Sl SUT1-GFP fusion construct is functional in sucrose uptake, and the uptake is inducible by GSSG. In each experiment, the SD of at least three independent uptake experiments is given.

The sucrose concentration was 1 mM in each experiment except for **(G)**.

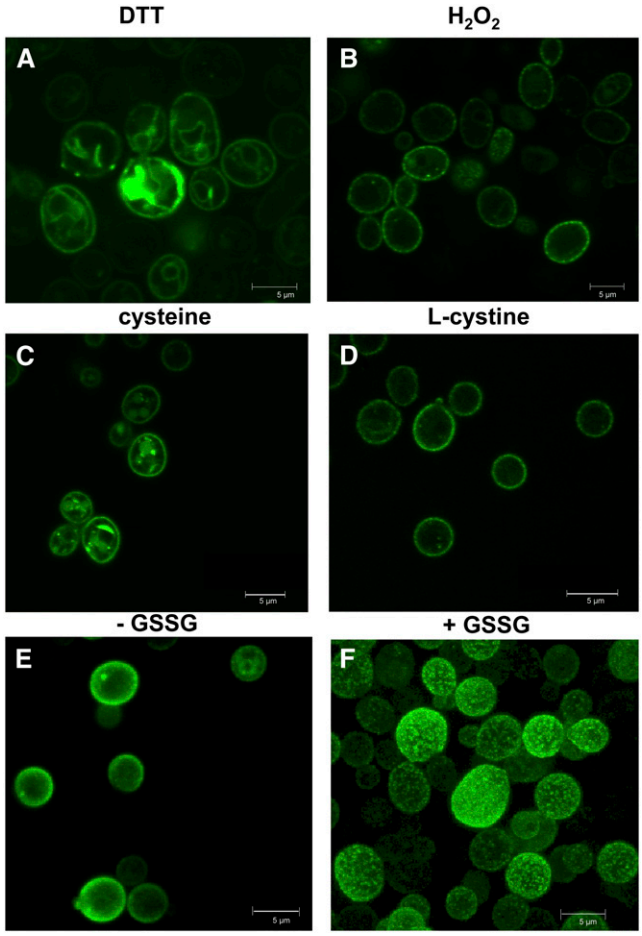

Figure 2. Analysis of Sl SUT1 Targeting in Yeast.

Confocal laser scanning microscopy of yeast cells expressing a Sl SUT1-GFP fusion construct in the strain SUSY7 using GFP-specific filter settings. Prior to the imaging analysis, yeast cells were treated for 30 min with 10 mM DTT **(A)**, 10 mM H_2O_2 **(B)**, 5 mM L-Cys **(C)**, or 5 mM L-cystine **(D)**.

(A) to **(D)** Single scans.

(E) and **(F)** Maximum projections of z-stacks of untreated yeast cells **(E)** or yeast cells incubated with 10 mM GSSG **(F)**.

St SUT1 are in the nA range (Boorer et al., 1996), we decided to perform these kinds of electrophysiological measurements with the homologous gene from maize (*Zea mays*), Zm *SUT1*, which is very well characterized and shows much higher sucrose-induced currents (in the μA range; Carpaneto et al., 2005). Two electrode voltage-clamp experiments were performed with *Xenopus laevis* oocytes expressing Zm *SUT1*, and sucrose-induced currents were recorded at various pHs with or without 1 mM GSSG (Figure 4B). At a holding potential of −70 mV and at acidic pH of 5.5, the sucrose-induced currents mediated by Zm SUT1 were twice as high in the presence of GSSG than in its absence (Figure 4B). Thus, we can exclude that neither changes of the ΔpH nor of the $\Delta\Psi$ are responsible for increased sucrose transport activity by SUT1 proteins. The redox control of SUT1 proteins is not due to secondary effects on the proton motive force.

St SUT1 Targeting in Plants

Immunolocalization of St SUT1 and Sl SUT1 in plants revealed an uneven distribution of the protein in fresh, longitudinal, unfixed stem sections. In Figure 5A, the projection of a z-stack of confocal images of two sieve elements is shown after decoration with St SUT1–specific antibodies. Unfixed in vitro–grown pollen tubes from tomato plants show a punctuated staining pattern upon immunolocalization of Sl SUT1 (Figure 5B).

Infiltrated tobacco (*Nicotiana tabacum*) leaves with a St SUT1-GFP fusion construct under control of the cauliflower mosaic virus 35S promoter did not only label the PM of epidermal cells but also endomembranes (Figure 5C). Coinfiltration with an ER marker protein (HDEL-mCherry) clearly demonstrates colocalization of St SUT1-GFP with the ER (Figure 5C).

As shown in yeast cells (Figure 3C), the targeting of the St SUT1-GFP construct in infiltrated tobacco leaves is sensitive to brefeldin A treatment (Figure 5D). Simultaneous incubation of infiltrated leaves with brefeldin A along with cycloheximide to inhibit de novo protein biosynthesis for 2 h leads to internal vesicle formation (Figure 5H). The half-life of the St SUT1 protein is very short (Kühn et al., 1997; He et al., 2008). Therefore, vesicles detected under these conditions are most likely due to endocytic events, rather than to inhibited vesicle fusion to the PM.

The effect of brefeldin A was also analyzed on embedded and fixed stem and leaf tissue. Prior to fixation, the potato plant material was preincubated with 50 μM brefeldin A for 1 h. Immunolocalization of St SUT1 revealed the presence of vesicle-like structures close to the PM of sieve elements both in longitudinal stem sections (Figures 5F and 5G) and in sieve elements of source leaf minor veins (Figures 5H and 5I).

Thus, targeting of St SUT1 to the PM of plant cells is most likely a reversible process, and the distribution of St SUT1 over the PM of mature sieve elements and pollen tubes is heterogeneous. Leaf samples without preincubation with brefeldin A show homogenous labeling of the sieve element PM (Figure 5J).

St SUT1 Is Detectable in the DRM Fraction from Potato

The presence of Sl SUT1-GFP fusion protein in lipid raft-like microdomains in yeast raises the question of whether SUT1 is a raft protein in plants. Because sphingolipid/cholesterol-rich liposomes were found to be insoluble in mild nonionic detergents such as Triton X-100 (TX100) at 4°C, the low-density TX100-insoluble membrane fractions are thought to reflect the in vivo composition of lipid microdomains (Simons and Ikonen, 1997; Brown and London, 1998). Lipid raft domains are thus defined as TX100-insoluble membranes and can easily be prepared from plant PMs (Mongrand et al., 2004; Lefebvre et al., 2007). Proteomics studies identified large numbers of raft proteins in plants; among them are proteins involved in signaling, cellular trafficking, or cell wall functions, whereas those involved in membrane transport are only poorly represented (Borner et al., 2005; Lefebvre et al., 2007). Evidence also exists for the

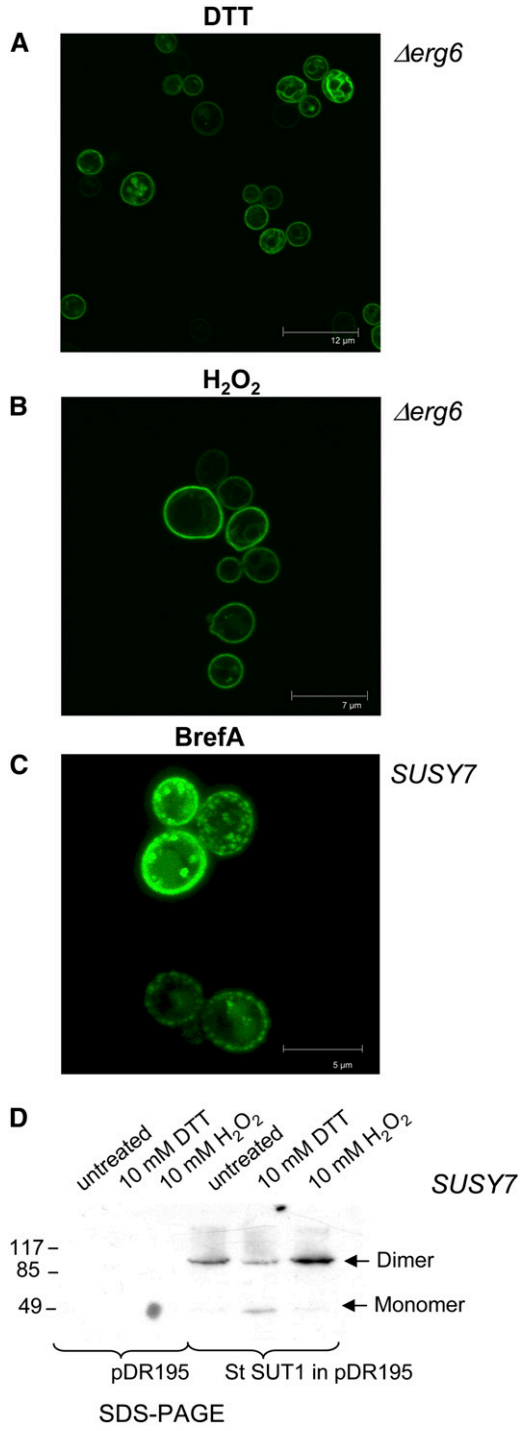

Figure 3. Heterologous Expression of SUT1 in Yeast.

(A) and **(B)** Sl SUT1-GFP expressed in the yeast ergosterol mutant Δ*erg6* strain was not detectable in lipid raft-like structures if treated with either 10 mM DTT **(A)** or 10 mM H_2O_2 **(B)**.

(C) Brefeldin A treatment of yeast cells expressing Sl SUT1-GFP. Internal vesicles are detectable upon 30 min of treatment with 50 μM brefeldin A when Sl SUT1-GFP is expressed in SUSY7.

(D) Immunodetection with St SUT1–specific antibodies of microsomal membrane proteins from yeast cells transformed with St SUT1 in the yeast expression vector pDR195 or with the empty vector. Yeast cells were preincubated for 30 min with 10 mM GSSG or 10 mM H_2O_2. Untreated membranes were loaded as controls, and equal amounts of protein were loaded. Arrows indicate SUT1 monomers and dimers.

presence of a complete PM redox system in the lipid rafts (Lefebvre et al., 2007). The DRM fraction from potato PMs was isolated via sucrose density ultracentrifugation (Figure 6A). Immunoblotting of proteins from DRMs revealed not only a band corresponding to the monomeric form of the St SUT1 protein, but an additional band corresponding to the molecular mass of the dimeric form (Figure 6B). By contrast, no St SUT1 protein was detectable in the soluble fraction containing the TX100-soluble proteins after 20 h of ultracentrifugation (Figure 6B). St SUT1 protein was enriched in the DRM fraction compared with the PM fraction when equal amounts of proteins were loaded (Figure 6C).

BN-PAGE Revealed a Dimeric Form of the St SUT1 Protein in Planta

To exclude that dimerization of St SUT1 observed in yeast is simply the consequence of heterologous overexpression of the protein, the St SUT1 protein was solubilized with *n*-dodecyl-β-maltoside (DDM) from plant PMVs. St SUT1 is a highly hydrophobic protein with a GRAVY score of 0.618 and a basic pI of 9.24. The effect of different DDM concentrations on St SUT1 migration behavior was analyzed. For this purpose, PMVs isolated from *S. tuberosum* source leaves were solubilized at DDM concentrations ranging from 0.2 to 2%, and the solubilized samples were subjected to BN-PAGE. St SUT1 protein was visualized by immunodetection using St SUT1–specific antibodies. St SUT1, which was isolated and electrophoretically separated under mild, native-like conditions at high protein concentrations (18 μg/μL) and at a high protein-to-detergent ratio (200 μg of total protein and 0.2% of DDM), yielded two distinct bands in BN-PAGE (Figure 7A). Two-dimensional SDS-PAGE, following BN-PAGE, clearly showed that both complexes separate into a 46-kD band, the apparent molecular mass of monomeric SUT1 (Figure 7B).

When St SUT1 was isolated and electrophoresed under more stringent conditions at a low protein concentration (0.2 μg/μL) and low protein-to-detergent ratio (20 μg of total protein and 2% DDM), only a single band, most likely the monomeric form, was observed. Thus, the equilibrium of the two St SUT1 species is shifted toward the low molecular mass fraction when increasing concentrations of DDM are used during preparation. Separation of the solubilized St SUT1 complex under native-like conditions overnight on a large (155-mm) 4 to 16% BN-PAGE gel also resulted in two bands that were recognized by the St SUT1–specific antibody (Figure 7B).

Similar results were obtained when PMVs were prepared from *S. lycopersicum*. Immunodetection after BN-PAGE revealed a monomeric and a dimeric band of the tomato sucrose transporter Sl SUT1 when PMs were solubilized with high

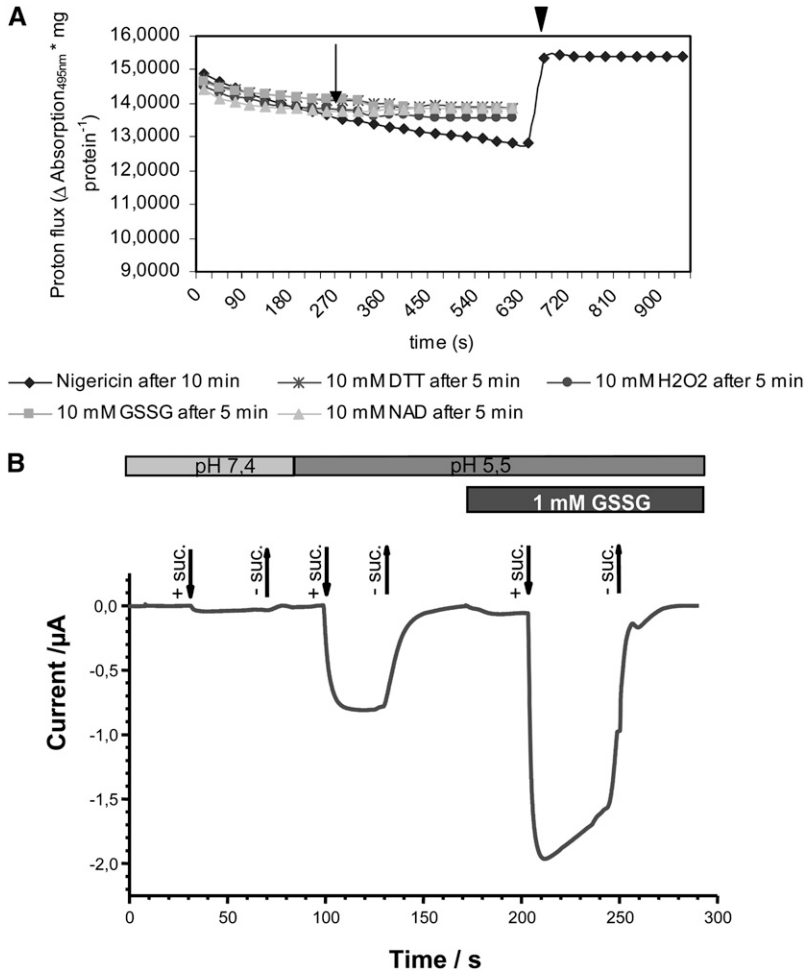

Figure 4. Proton Flux and Membrane Potential in Response to Redox Reagents.

(A) Proton flux in plant PMVs in response to redox reagents and nigericin. Proton pumping activities are unaffected in plant cells if redox reagents (NAD, GSSG, DTT, and H_2O_2) are supplied at equal pH after 5 min (arrow). Nigericin was applied after 10 min (arrowhead)

(B) Representative current recording from a *Xenopus* oocyte expressing Zm SUT1 at −70 mV holding potential. Transporter currents were evoked by perfusion at pH 7.4 or 5.5 in the presence or absence of 20 mM sucrose as schematically indicated by the perfusion scheme above the current trace, either in absence or presence of 1 mM GSSG. The experiment was conducted five times with oocytes from three different batches. The induction factor (current with 1 mM GSSG/current without GSSG) was 1.82 ± 0.17 (SD).

protein-to-detergent ratios (200 µg of total protein and 0.2% of DDM; Figure 7A).

The electrophoretic mobility on BN-PAGE of LacS, XylP, EIIMtl, and soluble marker proteins has been determined under conditions very similar to those used here (Heuberger et al., 2002). The approximate molecular masses of the lower and higher St SUT1 complexes were 99 and 213 kD, respectively, with respect to the soluble marker proteins. Heuberger et al. (2002) found that the migration of LacS, XylP, and other membrane transport proteins on BN-PAGE was overestimated by a factor of ~1.8 in comparison to the migration of soluble marker proteins. Using the conversion factor of 1.8, the molecular mass of St SUT1 is 54 kD for the lower and 119 kD for the higher migrating band. These values are in agreement with the calculated molecular mass of 55 kD for the monomer and 110 kD for the dimer (see Supplemental Figure 2 online).

Confirmation of St SUT1 Dimerization by Alternative Methods

o-Phtalaldehyde (OPA) has been widely used as a short (≈4 Å) chemical cross-linker. OPA reacts with thiols and primary amines yielding highly fluorescent 1-alkylthio-2-alkylisoindoles. The compound has been successfully used to determine the interaction between the subunits of Na^+, K^+-ATPases (Khan et al., 1996; Or et al., 1998). In this study, we have treated solubilized PMs from potato wild-type plants with OPA. We observed a cross-linked, dimeric St SUT1 protein complex after separation on a SDS-PAGE in wild-type plants (Figure 7C) and additional higher molecular complexes in samples with or without cross-linker. The monomeric form of the SUT1 protein appears as a double band, which is most likely due to posttranslational modifications. The activity of sucrose transporter proteins is known to

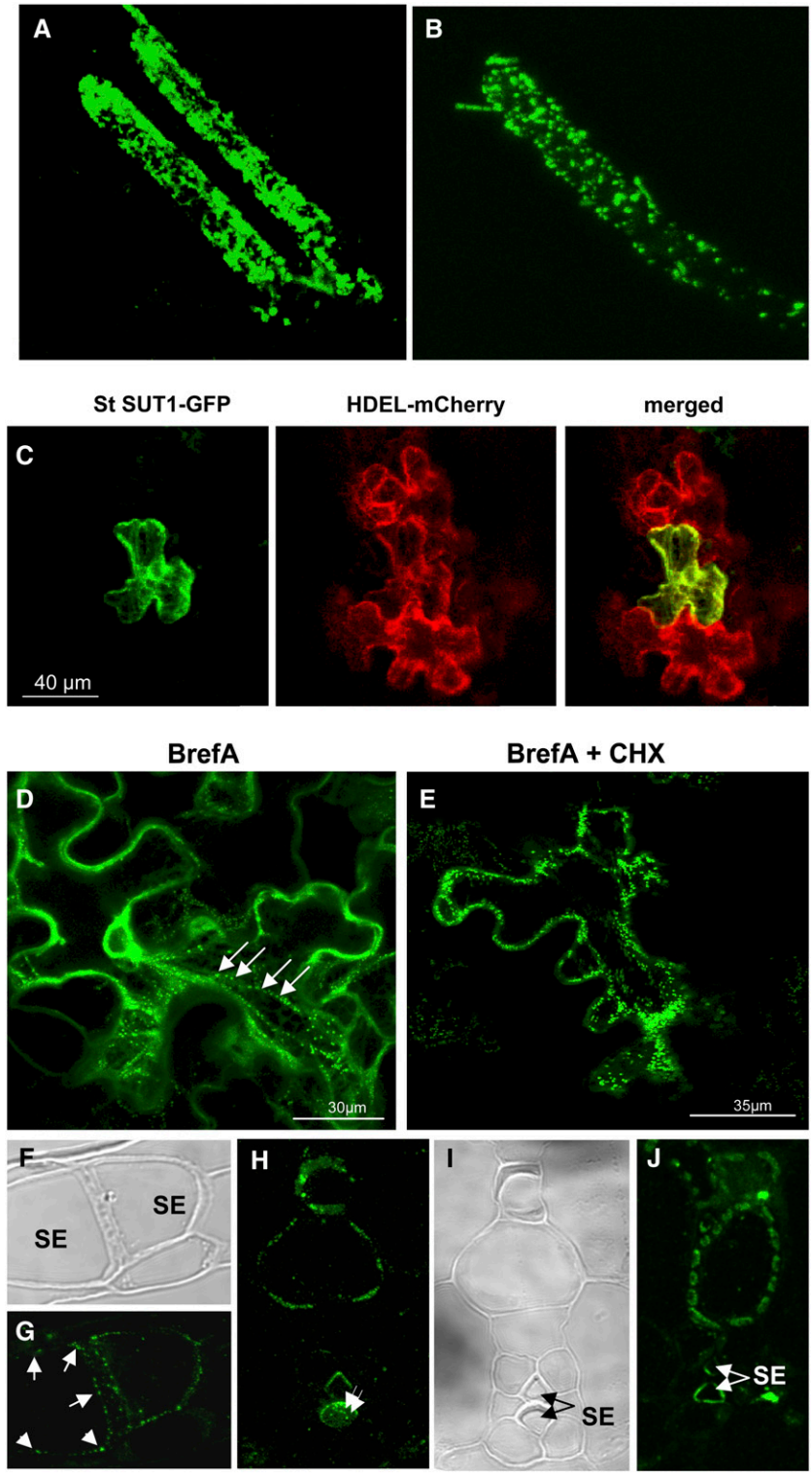

Figure 5. Localization of SUT1 in Plant Cells.

(A) Immunolocalization of St SUT1 in unfixed hand-cut longitudinal stem sections of potato plants using affinity-purified peptide antibodies shows uneven distribution of the St SUT1 protein at the sieve element PM. A maximum projection of a z-stack of confocal images is shown.
(B) Immunolocalization on unfixed in vitro–grown tomato pollen tubes treated with the above-mentioned antibody shows punctuate distribution of the SUT1 protein at the pollen tube PM.

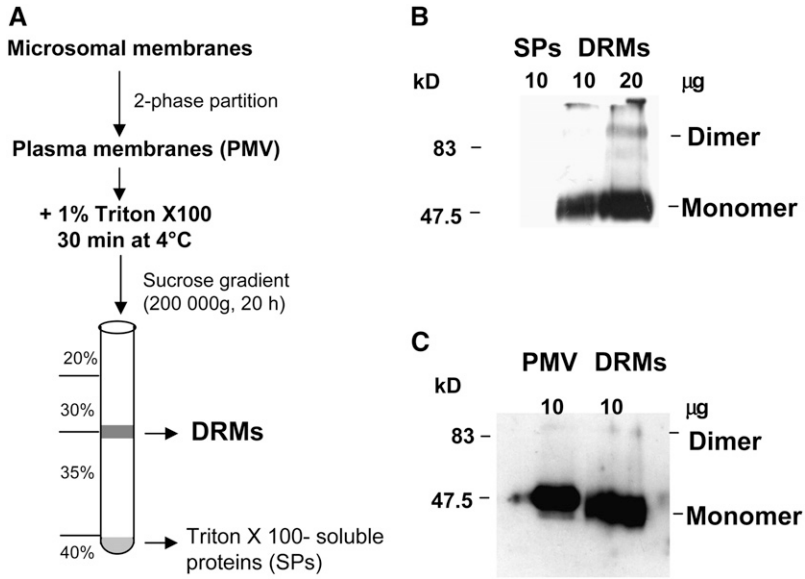

Figure 6. Analysis of the DRM Fractions from Potato Plants.

(A) The strategy for the preparation of the DRMs from potato PMs.
(B) Protein gel blot with DRMs (10 and 20 μg of proteins were loaded) and TX100-soluble proteins (SPs; 10 μg of proteins were loaded) after separation by SDS-PAGE. Immunodetection was performed with St SUT1–specific antibodies. DTT was omitted from the sample buffer. Note that the dimeric form of the protein is detectable in DRMs.
(C) Protein gel blot with PMVs prior to and after solubilization with TX100 shows enrichment of the St SUT1 protein compared with the DRM fraction (10 μg of proteins were loaded in each lane).

be regulated via phosphorylation/dephosphorylation (Roblin et al., 1998). Reducing agents like DTT or β-mercaptoethanol led to dissociation of the dimeric protein (Figure 7D), whereas in the absence of DTT, some dimeric St SUT1 was detectable after SDS-PAGE (Figure 7D). Thus, in plants, St SUT1 is readily cross-linked via one or more native Cys pairs that must reside at the dimer interface.

To test whether the complex that was formed by chemical cross-linking corresponds to dimeric St SUT1 or St SUT1 in complex with another protein, immunoprecipitation with purified St SUT1–specific antiserum was performed. Protein gel blot analysis of the precipitated proteins with SUT1-, SUT2-, and SUT4-specific antibodies revealed the monomeric and the dimeric form of SUT1 using SUT1 antibodies (Figure 7E) but no immunoreacting band with SUT2 or SUT4 antibodies (data not shown). Thus, immunoprecipitation together with protein gel blot analysis argue for homodimerization of St SUT1 in planta.

Figure 5. (continued).

(C) Colocalization of a St SUT1-GFP construct under control of the cauliflower mosaic virus 35S promoter (green) with an ER tracker HDEL-mCherry (red) after infiltration of *Nicotiana benthamiana*. The merged picture shows that St SUT1-GFP is not only targeted to the PM but also to the ER (yellow).
(D) Tobacco leaves infiltrated with a St SUT1-GFP fusion construct 48 h after infiltration. Leaves were treated for 30 min with 50 μm brefeldin A. A maximum projection of a time series is shown.
(E) The same St SUT1-GFP construct used in **(D)** analyzed after incubation of infiltrated tobacco leaves with 50 μM brefeldin A and 10 μM cycloheximide (CHX) after 2 h. A maximum projection of a time series is shown.
(F) Transmission electron micrographs of a longitudinal semithin section of embedded potato stem tissue used for immunolocalization shown in **(G)**.
(G) Immunolocalization of St SUT1 in potato stems that were preincubated prior to fixation with 50 μM brefeldin A for 1 h. Immunodetection was performed with affinity-purified St SUT1 peptide antibody and an FITC-coupled secondary antibody.
(H) Minor vein of potato source leaf cross section of embedded material preincubated prior to fixation with 50 μM brefeldin A. The same immunolocalization procedure was performed as described for **(G)**.
(I) Transmission electron micrograph of the semithin section used for immunolocalization shown in **(H)**.
(J) Immunolocalization of St SUT1 in phloem sieve elements without pretreatement with brefeldin A shows homogenous distribution of the protein over the sieve element PM. SE, sieve elements.
In **(D)**, **(G)**, and **(H)**, arrows label endocytic vesicles.

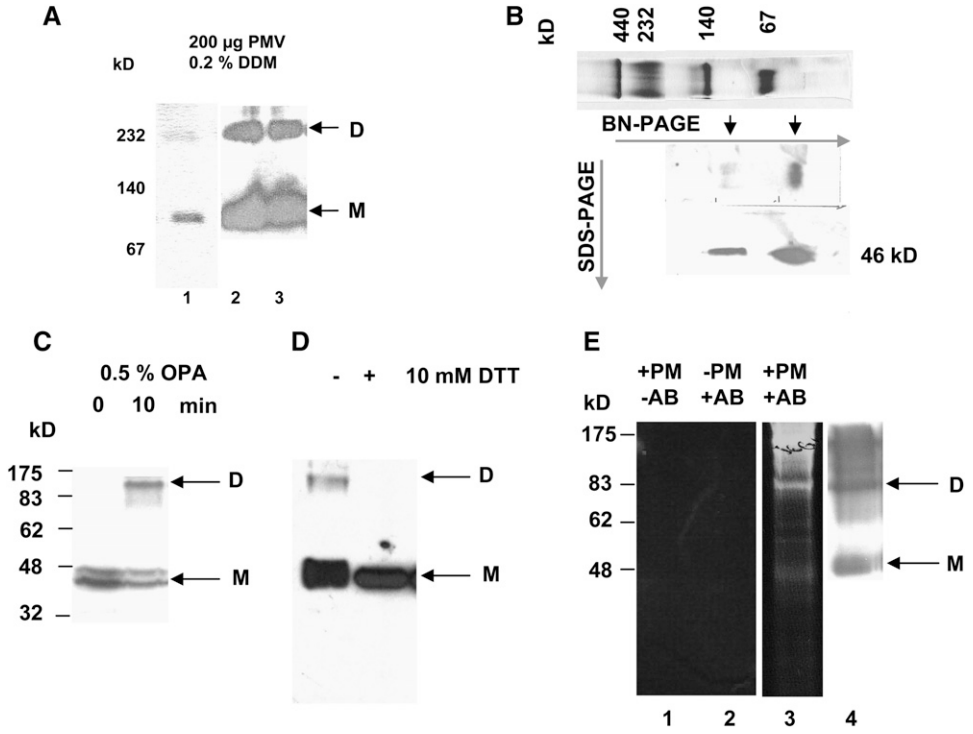

Figure 7. Analysis of St SUT1 Oligomerization in Planta.

(A) St SUT1–specific immunodetection of SUT1 in tomato and potato PMs solubilized with DDM and separated with BN-PAGE. Protein and detergent concentrations are indicated. PMV from potato (lanes 2 and 3, identical samples) and tomato (lane 1) plants were loaded and separated in a small (60 mm) protein gel for 3.5 h.

(B) Two-dimensional gel electrophoresis of potato wild-type PMs. In a first dimension, potato PMVs were separated in a large (155 mm) protein gel overnight under native conditions. The BN-PAGE band was separated in the second dimension by SDS-PAGE, and both dimensions were immunoprobed with St SUT1–specific antibodies. The marker proteins from the first dimension gel under native conditions are shown above. Arrows label the immunoreacting bands of the SUT1 dimer and monomer.

(C) St SUT1–specific immunodetection of SUT1 in solubilized potato PMs cross-linked with OPA for the indicated time and separated by SDS-PAGE.

(D) St SUT1–specific immunodetection of SUT1 in microsomal membranes (15 μg) prepared from potato wild-type plants and separated by SDS-PAGE in the presence or absence of 10 mM DTT.

(E) Immunoprecipitation of SUT1, using a SUT1-specific antibody, and separation by SDS-PAGE revealed a high molecular band corresponding to the SUT1 dimer (lane 3), as shown by immunodetection (lane 4). Controls: elution from solubilized PMs purified with Sepharose A without antibody (lane 1), elution from Sepharose with anti-St SUT1 antibody without solubilized PMs (lane 2). Gels were stained with SYPRO Ruby (lane 1 to 3), and the protein gel blot was performed with SUT1 antibody (lane 4). Note that immunoglobulins are also detectable in the gel after immunoprecipitation. AB, antibody; M, monomers of SUT1; D, dimers of SUT1.

Homodimerization of St SUT1 in Plant Cells Visualized by BiFC

The technique of BiFC for visualization of protein–protein interactions in plant cells is based on the formation of a fluorescent complex from two nonfluorescent fragments of the yellow fluorescent protein (YFP), which are brought together by association of interacting proteins fused to different halves of the YFP molecule (Walter et al., 2004). Various complementary sets of expression vectors, which enable protein interaction studies in transiently or stably transformed cells, are available for the visualization of the subcellular sites of protein interactions (Walter et al., 2004). BiFC was used to confirm the capacity of Sl SUT1 to form homodimers in transiently or stably transformed plant cells (Figures 8A and 8B). As a negative control, coexpression of Sl *SUT1* together with the PM potassium channel TPK4 from *Arabidopsis thaliana* (kindly provided by K. Czempinsky) in the BiFC vector 35S-SPYNE did not result in reconstitution of a fluorescent YFP molecule (Figure 8C).

Oligomerization in Transgenic Plants with Reduced St SUT1 Expression

Immunolocalization of St SUT1 in wild-type potato plants showed the highest expression of St SUT1 in sieve elements (Kühn et al., 1997), but it cannot be excluded that St SUT1 is also expressed in cells other than phloem (Lemoine et al., 1996; Weise et al., 2008). Antisense plants with phloem-specific inhibition of St SUT1 expression using the companion cell-specific

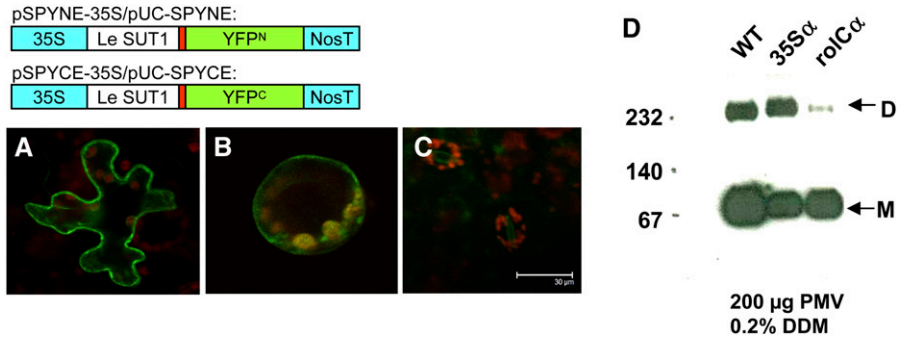

Figure 8. SUT1 Oligomerization in Transiently or Stably Transformed Plants.

(A) Homodimerization of Sl SUT1 visualized via split YFP in transiently transformed tobacco leaves. Sl SUT1 fusion constructs with either the N-terminal or C-terminal part of YFP, cloned in the binary vectors 35S-SPYNE and 35S-SPYCE, respectively, were used for transformation of *Agrobacterium tumefaciens*. YFP fluorescence in *Agrobacterium*-infiltrated tobacco leaves was detected 48 h after infiltration of Sl SUT1-SPYNE and Sl SUT1 SPYCE.
(B) YFP fluorescence of tobacco protoplasts transformed with pUC derivatives Sl SUT1-pUC-SPYNE and Sl SUT1-pUC-SPYCE was detected 24 h after protoplast transformation.
(C) As a negative control, the *Arabidopsis* potassium channel TPK4 in SPYCE was coinfiltrated with Sl SUT1-SPYNE. YFP fluorescence is visible as green and chlorophyll autofluorescence as red.
(D) Analysis by BN-PAGE of transgenic plants with reduced expression of St SUT1. BN-PAGE of potato wild-type and St SUT1 antisense potato plants (35S- or *rolC*-promoter) after immunodetection with St SUT1–specific antibodies. M, monomer; D, dimer.

rolC promoter showed a strong phenotype, including leaf chlorosis, reduced growth, and reduced development of sink organs (Kühn et al., 1996). BN-PAGE of PMs prepared from phloem-specific inhibited St *SUT1* antisense plants revealed a strong reduction of the dimeric band compared with wild-type plants (Figure 8D), whereas in antisense plants with constitutive reduction of St *SUT1* expression, only the monomeric form of the protein was reduced. The dimer-to-monomer ratio in potato plants ranges between 0.5 and 0.7. In constitutively inhibited St *SUT1* antisense plants, the ratio is shifted toward values above 0.7, whereas in *rolC* antisense plants, the dimer-to-monomer ratio is lowered to values between 0.1 and 0.3. Phloem-specific *SUT1* inhibition apparently leads to reduction of mainly the dimeric but not of the monomeric form of the protein.

DISCUSSION

Redox Control of Transporter Activity

All previously reported SUT1-mediated sucrose uptake measurements most probably correspond to the monomeric form of the protein (Riesmeier et al., 1993; Boorer et al., 1996). We show in this report that in the presence of oxidizing agents, sucrose uptake can be stimulated at least 10-fold (Figure 1). Organic redox reagents, such as oxidized glutathione and L-cystine, strongly enhanced St SUT1–mediated sucrose uptake, and the increased rates of transport were reached immediately after the addition of the oxidants. This increase is due to an increase in the V_{max}, while the K_m remained constant. Oxidation of SUT1 proteins might be a posttranslational regulatory mechanism allowing an increased flexibility of the transporter. The redox-dependent activation of the St SUT1 and Zm SUT1 proteins was an immediate effect, as shown by sucrose uptake studies in yeast as well as in *Xenopus* oocytes (Figures 1 and 4). The increased targeting of Sl SUT1-GFP to the PM in the presence of GSSG or other oxidizing agents took much longer, and the final partitioning was reached only after 30 min of incubation with the oxidants (Figure 2). Thus, the strong increase in sucrose transport activity is not explained solely by more efficient targeting of the protein to the PM under oxidizing conditions. We suggest rapid conformational changes in the protein induced either by inter- or intramolecular disulfide bridges as the main contributors to the rise in the uptake activity. Interestingly, the redox-dependent activation by oxidized glutathione showed a $K_{0.5}$ of 3 mM, which is close to the physiological concentration of glutathione in the phloem sap of several plants (Szederkényi et al., 1997). Reversible redox regulation is a possibility to transiently inhibit or activate sucrose transport activity.

Redox Control of Membrane Protein Targeting

It is known for other membrane proteins that targeting to the PM can be affected by the cellular redox state. For instance, disulfide bridges in the Na^+, K^+-ATPase play a role in the assembly of the protein when it exits the ER and travels to the PM, where the protein is catalytically active (Laughery et al., 2003). For several other membrane proteins that are able to form multimers, oligomerization was shown to be a prerequisite for the export from the ER and for correct PM targeting (Gao and Dean, 2000; Liang et al., 2004; Salahpour et al., 2004). Intra- and intermolecular disulfide bridges together were shown to be important for the structure and functions of the human multidrug resistance transporter ABCG2 (Henriksen et al., 2005). In mitochondria, a disulfide relay system catalyzes the import of proteins into the intermembrane space by an oxidative folding mechanism (Mesecke et al., 2005), and for immunoglobulins free thiol groups play a role in the transport through the secretory pathway and the

quality control (Alberini et al., 1990; Fra et al., 1993). For St SUT1, it is already described that the sucrose transport activity can be abolished by addition of thiol modifying agents such as pCMBS or NEM (Riesmeier et al., 1992).

In yeast cells, the oxidation of St SUT1 increased its targeting to the PM as shown by the GFP fusion constructs and the protein's organization in lipid raft-like structures (Figures 2B, 2D, and 2F). Such lipid domains in yeast cells are known for endogenous yeast transporters as well as for heterologously expressed plant membrane proteins (Malinska et al., 2003; Grossmann et al., 2006). On the contrary, endogenous yeast H^+-ATPase Pma1p was found in membrane compartments called MCP (for membrane compartment occupied by Pma1p), exhibiting a network-like pattern (Grossmann et al., 2007). Thus, it is unlikely that St SUT1 colocalizes with the endogenous *pmf*-producing Pma1p. Nevertheless, the increase in *pmf*-dependent sucrose uptake was dramatic and paralleled the increased repartitioning of St SUT1 at the PM (Figures 1 and 2). Lipid rafts have been proposed to facilitate oligomeric interactions to separate signaling components or to affect the function of membrane proteins via a different lipid environment (Grossmann et al., 2006). Interestingly, the concentration of the Sl SUT1-GFP fusion construct in lipid raft-like structures is disturbed in the yeast ergosterol *erg6* mutant, whereas the increase in PM targeting in the presence of oxidizing agents can still be observed in the Δ*erg6* mutant (Figures 3A and 3B), arguing for two distinct phenomena.

The presence of St SUT1 dimers in the detergent-resistant membrane fraction of potato PMs is a strong argument to consider St SUT1 as a plant raft protein. It cannot be excluded that St SUT1 organization in membrane raft-like compartments is related to the cellular trafficking of the protein and the regulation of its activity via redox regulators. Recently, a proteomic approach with root PMs from *Medicago truncatula* revealed the presence of a complete raft-associated redox system (Lefebvre et al., 2007).

Oligomerization and PM Targeting

It is described for several plant membrane proteins that oligomerization is a prerequisite for ER export and/or PM targeting. Tetramerization of the potassium channel KAT1 via a diacidic motif is needed for ER export (Mikosch et al., 2006), and recent studies on aquaporins from maize revealed the requirement for heterodimerization to be exported from the ER and to be targeted to the PM (Maurel, 2007). Further localization studies in St SUT1 in plants will answer the question whether redox-dependent targeting of the sucrose transporter is restricted to yeast cells or can also be observed in plant cells.

In a recent study, it was shown that expression of a membrane-anchored fluorescent protein under control of the companion cell-specific At SUC2 promoter illuminates the sieve element PM in *Arabidopsis* and tobacco (Thompson and Wolniak, 2008). It is discussed whether the transport of the membrane-anchored protein occurs through the desmotubules connecting the ER network of the companion cells and the sieve elements followed by additional vesicular transport to the sieve element PM. Fluorescence of the membrane-anchored fusion protein is also detected in vesicle-like structures in the mature sieve elements (Thompson and Wolniak, 2008). A similar route is now suggested for the targeting of St SUT1.

Oligomeric State of St SUT1 in Yeast and Plants

The potential of St SUT1 to form homodimers in plant cells was shown by BN-PAGE and by YFP reassembly (BiFC assay) in infiltrated tobacco leaves and protoplasts. Heterologous expression of St SUT1 in *Saccharomyces cerevisiae* also revealed the potential of the protein to dimerize. Clearly, additional plant-derived factors are not required for homodimerization. The monomer to dimer equilibrium of the purified St SUT1 protein depends on the concentration of the detergent used during the purification procedure.

Quantification of the affinity of homo- and heterodimerization of the sucrose transporters from tomato was performed by β-galactosidase activity assay and showed that the affinity of homooligomers of two SUT1 subunits is twice as high than the heterooligomerization between SUT1 and SUT4, and 4 times higher than between SUT1 and SUT2 (Reinders et al., 2002). Therefore, the formation of SUT1 homodimers is more likely than the formation of heterodimers. However, formation of heterodimers cannot be excluded by the presented experiments.

St SUT1 Oligomerization in Transgenic Plants

Under native-like conditions, a phloem-specific reduction of the dimeric form of the St SUT1 protein was detectable in St *SUT1* antisense plants, whereas constitutively inhibited antisense plants showed only reduction of the monomer. These observations argue for the presence of dimeric St SUT1 in the phloem, where the protein's main function is the secondary active transport of sucrose against a steep concentration gradient into the sieve element lumen. Apparently, the ability to oligomerize is related to the cell type where St SUT1 is expressed: the monomeric St SUT1 being dominant in cells other than phloem tissue, while the dimeric St SUT1 is preferentially present in phloem sieve elements.

Redox Control in Mature Sieve Elements

The thiol-disulfide status of plant cells has fundamental effects on plant metabolism (Kolbe et al., 2006), and the activity of many sucrose metabolizing enzymes shows redox-dependent regulation. For instance, the key enzyme in starch synthesis, the ADP-glucose pyrophosphorylase (AGPase), is shown to be redox regulated and active in the monomeric but inactive in the dimeric form (Hendriks et al., 2003). Recent work revealed a redox-dependent posttranslational regulation of the sucrose-metabolizing sucrose synthase, which acts as multimeric complex that is substrate inhibited by fructose (Marino et al., 2008). The St SUT1 protein has been localized and is functional in phloem sieve elements (Kühn et al., 1997), and all three known sucrose transporters from potato follow a circadian clock oscillation (Chincinska et al., 2008). One of the major proteins in the phloem sap of rice (*Oryza sativa*) is thioredoxin h, a plant thiol-disulfide oxidoreductase (Ishiwatari et al., 1995). Thioredoxin h is discussed to contribute to a light-dependent long-distance thiol

signal being generated in leaves and thereby connecting metabolic processes in sink organs with photosynthetic activity in source organs (Balmer et al., 2006). Thioredoxin h is also discussed to play a role in circadian clock regulation and is shown to be light induced (Lemaire et al., 1999, 2002).

The phloem-specific P-proteins PP1 and PP2 from *Cucurbitaceae* are redox-sensitive proteins whose precipitation could indicate a drop of the redox potential in the sieve elements. They are responsible for redox-dependent gelation of the phloem sap upon application of oxidative agents (Alosi et al., 1988).

In mature sieve elements, a complete antioxidant defense system has been detected (Walz et al., 2002), and activity of superoxide dismutase, monodehydroascorbate reductase, and peroxidase could be shown. In addition, activity of several antioxidant enzymes, such as superoxide dismutase, dehydroascorbate reductase, and peroxidase, could be demonstrated in phloem exudates. Ascorbate and glutathione, as well as thioredoxin and glutaredoxin, are also detectable in the phloem sap (Szederkényi et al., 1997; Franceschi and Tarlyn, 2002). Thus, all requirements of a systemically translocated redox signal via the phloem translocation stream are met.

The phloem sap is highly reducing, and a protective role for damage by oxidative stress is provided (Franceschi and Tarlyn, 2002). Since the apoplasmic space is less reducing than the phloem sap in the lumen of the sieve elements, it is likely that disulfide bonds might be formed extracellularly. The redox potential of the apoplasmic space undergoes drastic changes upon various forms of biotic and abiotic stresses. It is known that pathogens are able to induce changes in the antioxidant status in the apoplast (Bolwell et al., 2001; Hu et al., 2005; Diaz-Vivancos et al., 2006) and that dehydroascorbate, glutathione, superoxide dismutase, catalase, ascorbate peroxidase, glutathione reductase, monodehydroascorbate reductase, and dehydroascorbate reductase are present in the apoplast (Vanacker et al., 1998). An inducible glutathione *S*-transferase was also localized in the apoplast of soybean hypocotyls (Flury et al., 1996).

The relative amount of GSSG has for a long time been overestimated. Recently, the dynamic live imaging of the glutathione redox potential revealed nanomolar changes in GSSG against a backdrop of millimolar GSH on a short time scale leading to the assumption that GSSG might act as a second messenger (Gutscher et al., 2008).

We conclude that redox-dependent posttranslational modification of SUT1 induces an immediate increase in sucrose transport capacity and affinity. PM targeting of SUT1 in yeast as well as in plants is reversible by application of brefeldin A. In yeast cells, SUT1-GFP accumulates in microdomains, and in plants, St SUT1 comigrates with the DRM fraction in a sucrose gradient. It is suggested that raft association of St SUT1 might be related to oligomerization and/or PM recycling and endocytosis of the protein.

The redox sensitivity of the sucrose transporter SUT1 might represent an additional possibility to transduce long-distance information about the oxidative status in leaves in form of the sucrose molecule. Thus, we present one further possibility of how the transformation between redox signaling and sucrose signaling might be achieved in higher plants.

METHODS

Plant Growth Conditions

Solanum tuberosum DÈsirÈe and *Solanum lycopersicum* Moneymaker were grown in the greenhouse in a cycle of 16 h light (22°C) and 8 h darkness (15°C) in 60% humidity. Additional illumination was provided by high-pressure sodium lamps (SON-T Green Power) and metal halide lamps (MASTER LPI-T Plus; Philips). Generation of phloem specifically and constitutively inhibited St *SUT1* antisense potato plants was described previously (Riesmeier et al., 1994; Kühn et al., 1996).

Construction of Split YFP Plasmids

Split YFP experiments were basically performed as described (Walter et al., 2004). Sl SUT1 was amplified by PCR with Phusion proofreading polymerase (New England Biolabs) using the following primers: Sl SUT1 was cloned via *Xba*I and *Kpn*I in the pUC-derived SPYNE vector using the forward primer 5′-AGAATCTAGAATGGAGAATGGT-3′ and reverse primer 5′-ATTTGGTACCATGGAAACCGCC-3′, and via *Xba*I and *Sma*I in the 35S-SPYNE vector using the above-mentioned forward primer together with the primer 5′-TTCCCGGGATGGAAACCGCCCAT-3′. PCR products were analyzed by restriction digestion and partial sequencing. All split YFP vectors (pUC-SPYNE, pUC-SPYCE, 35S-SPYNE, and 35S-SPYCE) were kindly provided by Klaus Harter (Walter et al., 2004). Fusion of Sl SUT1 to GFP used for uptake and targeting experiments in yeast was described previously (Reinders et al., 2002). The Sl SUT1-GFP fusion was cloned via GATEWAY technology in the vector pDR196-GATEWAY kindly provided by D. Rentsch (Bern, Switzerland) and used for transformation of the *erg6* yeast mutant (Matα, his3Δ1, leu2Δ0, lys2Δ0, ura3Δ0YML008c::kanMX4; Euroscarf). The St SUT1-GFP construct used for tobacco (*Nicotiana benthamiana*) leaf infiltration experiments was generated by cloning the St SUT1 coding region in a pCF203-derived plasmid with a modified multiple cloning site (detailed description in Chincinska et al., 2008). St SUT1 was amplified with primers with restriction sites for *Kpn*I and *Eco*RV and cloned in the modified pCF203 linearized with *Bam*HI, blunted, and redigested with *Kpn*I.

Transformation of Protoplasts and Infiltration of *N. benthamiana* and *S. tuberosum* Leaves

Transformation of tobacco protoplasts with pUC-derived BiFC plasmids was basically performed as described (Andrews and Curtis, 2005) using Sl SUT1-pUC-SPYNE and Sl SUT1-pUC-SPYCE. Transient expression of 35S-BiFC constructs in infiltrated tobacco leaves was performed as described (Walter et al., 2004) using Sl SUT1-35S-SPYNE, Sl SUT1-35S-SPYCE, and TPK4-35S-SPYCE (kindly provided by Katrin Czempinski). Fluorescence was detected 24 to 48 h after infiltration with a confocal laser scanning microscope (TCS SP2; Leica) using YFP-specific filter settings and excitation at 514 nm.

Isolation of Plant PMVs

Plant PMVs were purified from a microsomal fraction from tomato or potato plants by two-phase partitioning as described (Larsson, 1985). The crude PM fraction was enriched using an aqueous two-phase system (6.6% PEG/6.6% Dextran) (Bush, 1989), and the total protein concentration was estimated by the Lowry method (Bio-Rad).

The proton flux in response to H_2O_2, DTT, GSSG, NAD, and nigericin (10 mM in each case) was measured with inside out PMVs after treatment with Bri58 by acridine orange quenching at 495 nm as described elsewhere (Palmgren and Sommarin, 1989; Palmgren, 1990).

The DRM fraction was prepared exactly as described elsewhere (Morel et al., 2006). PMs were resuspended in buffer A containing 50

mM Tris-HCl, pH 7.4, 3 mM EDTA, and 1 mM DTT and treated with 1% TX100 (w/v) for 30 min on ice with gentle shaking every 10 min. Solubilized membranes were placed at the bottom of a centrifuge tube and mixed with 60% sucrose (w/w) to reach a final concentration of 48% (w/w) and overlaid with a discontinuous sucrose gradient (40, 35, 30, and 20% [w/w]). After centrifugation for 20 h at 100,000*g*, a ring of TX100-insoluble membranes was recovered at the 30 to 35% interface, diluted in buffer A, and centrifuged for 4 h at 100,000*g*. The pellet was resuspended in buffer A, and protein concentrations were determined using the Lowry method with BSA as the standard.

Isolation of the Microsomal Fraction from Yeast Cells

Yeast cells were harvested by centrifugation and resuspended in 1 mL of cold protein extract lysis Buffer (50 mM Tris-Cl, pH 7.5). After the addition of 300 μL of glass beads, cells were disrupted mechanically by vigorous vortexing for 7 × 30 s and cooled on ice between vortexing. Membranes were collected by ultracentrifugation at 80,000 rpm for 60 min at 4°C (TLA 110 rotor; Beckman).

Gel Electrophoresis and Protein Gel Blotting

SDS-PAGE was performed in accordance to Laemmli (1970), and protein gel blotting was performed using a semidry electroblotter (Hoefer) as described (Bjerrum and Heegaard, 1988). Protein gel blot analysis was performed as described previously (Kühn et al., 1996). BN-PAGE was performed according to Schägger et al. (1994) with few alterations. Acrylamide gradient gels (5 to 20%) with 4% overlay were run at 35 V for 1e h using cathode buffer (50 mM Tricine-Cl and 15 mM Bis Tris-Cl, pH 7.0) with 0.02% Coomassie Brilliant Blue G and continued for 3 h at 200 V with cathode buffer without Coomassie. Large (155 mm) gradient gels had a 4 to 16% acrylamide concentrations and were run for 16 h (Figure 7B). All steps were performed at room temperature. Samples were prepared by the addition of 0.25 volumes of a 5% solution/suspension of Serva blue G 250 in 500 mM ε-amino-*n*-caproic acid and 100 mM Bis-Tris-Cl at pH 7.0, resulting in 1% Coomassie Brilliant Blue G, final concentration. Proteins were blotted to a polyvinylidene difluoride membrane (0.45 μm; Millipore) in the same buffer using the semidry approach as referenced above. Immunodetection with an anti-St SUT1 antibody was performed as described previously (Kühn et al., 1997). Calibration of the St SUT1 molecular mass was performed with a small 5 to 20% acrylamide gradient gel after 3 and 5 h run at 200 V in the presence of known marker proteins (Thyroglobulin, Ferritin, Catalase, Lactate Dehydrogenase, and BSA) according to Heuberger et al. (2002).

Chemical Cross-Linking and Immunoprecipitation

Chemical cross-linking experiments were performed with isolated PMVs from potato wild-type plants with the OPA cross-linker molecule as described (Or et al., 1998), and 0.5 or 1 μL of 0.5% OPA was applied for 10 min at 30°C to 170 μL PMV (2 mg/mL). The reactions were quenched with 25 μL of 1 M Tris-Cl, pH 8.0, for 20 min at 30°C. After ultracentrifugation at 4°C for 20 min at 80,000 rpm (TLA 110 rotor; Beckman) the pellets were resuspended in sample buffer used for SDS-PAGE analysis. Immunoprecipitation was performed using affinity-purified St SUT1–specific antibodies coupled to Sepharose A (Sigma-Aldrich) according to the manufacturer's protocol.

^{14}C-Sucrose Uptake in Yeast Cells

Uptake experiments were performed with yeast strain SUSY7 [Matα, suc2Δ::URA3, mal0, trp1, LEU2::P ADH1-SUSY (YIP128 A2)] as described elsewhere (Weise et al., 2000). Yeast cells were grown in liquid minimal medium containing glucose to an OD_{600} of 0.8 to 1.0. Cells were collected by centrifugation, washed in 25 mM sodium phosphate, pH 7.0, and suspended in the same buffer to an OD_{600} of 50. Cells were pretreated for 5 min with redox reagents, and uptake assays were initiated by adding glucose to a final concentration of 10 mM to yeast cells, 1 min prior to the addition of ^{14}C-sucrose (specific activity of the ^{14}C-sucrose stock: 600 mCi/mmol; purchased from Amersham Biosciences). Cells were collected by vacuum filtration on a 0.45-μm cellulose nitrate filter (Whatman) and washed with ice-cold 25 mM Na-phosphate supplemented with 10 mM sucrose. Radioactivity was determined in a liquid scintillation counter. Uptake experiments were performed at neutral pH to ensure stability of redox reagents if not indicated otherwise. Final concentrations of sucrose were adjusted to 1 mM with unlabeled sucrose in all experiments if not indicated otherwise (i.e., Figures 1E and 1F). When appropriate, 10 μM CCCP was added 1 min before the start of the transport measurements.

Microscopy of Yeast Cells

Yeast cells were harvested by gentle centrifugation (3 min, 1000*g*) and immobilized either with 0.1% agarose or by settling on adhesion slides (Starfrost) for a few minutes and analyzed with GFP-specific filter settings with a CLSM TCS SP2 microscope (Leica). Redox reagents were added at 10 mM final concentration, 30 min before the analysis (Cys and cystine at 5 mM final concentration). *O*-phtahladehyde (0.05%) and methyl-β-cyclodextrin (30 μM) was applied 30 min before analysis.

Immunolocalization

Immunolocalization experiments were performed with fresh in vitro–grown tomato pollen tubes using SUT1-specific affinity-purified peptide antibodies as described earlier (Hackel et al., 2006). Immunolocalization with longitudinal stem sections from potato plants was performed with fresh and unfixed hand-cut material as described by Wang et al. (1995). Fresh hand sections were blocked for 30 min with PBS-milk 2.5% (w/v) and incubated overnight in the St SUT1 antiserum, washed for 30 min in PBS milk 2.5% (w/v), and incubated for 1 h in FITC-labeled secondary antibody (Wang et al., 1995).

Embedded tissue was immunostained according to Kühn et al. (1997). Before fixation and dehydration, some tissue samples were preincubated for 1 h with 10 μM brefeldin A or with 10 μM brefeldin A and 10 μM cycloheximide. Confocal images were taken with the TCS SP2 confocal laser scanning microscope (Leica) using FITC-specific filter settings and excitation at 488 nm or in case of transmission pictures of semithin sections using the transmission photomultiplier (PMTTrans).

Electrophysiology in *Xenopus laevis* Oocytes

The cDNA encoding the sucrose transporter Zm SUT1 from *Zea mays* was subcloned in the high-expression vector pGEM-HE, which is based on pGEM-3Z (Promega) containing 5′ and 3′ untranslated sequences of the *Xenopus* β-globin gene flanking the transporter cDNA (Liman et al., 1992). After plasmid linearization with *Nhe*I, cRNA synthesis was performed using the T7 mMessage mMachine kit (Ambion). Oocytes were obtained by partial ovarectomy from anesthetized *Xenopus* females, followed by treatment with Collagenase 1A (Sigma-Aldrich). Each oocyte was injected with 25 ng Zm SUT1 cRNAs and stored in ORI buffer (contents in mM: 110 NaCl, 5 KCl, 1 $MgCl_2$, 2 $CaCl_2$, and 5 HEPES, pH 7.4) containing 50 mg/L gentamycin at 18°C for 3 to 4 d. Currents were recorded by a two-electrode voltage clamp using a Turbotec 10CX amplifier (NPI instruments) and pClamp 7 software (Axon Instruments) at 21 to 23°C. Solutions used were as follows: Solution A (contents in mM: 100 NaCl, 2 KCl, 2$MgCl_2$, 0,2 $CaCl_2$, and 10 HEPES/TMA, pH 7.4), Solution B (contents in mM: 100 NaCl, 2 KCl, 2$MgCl_2$, 0,2 $CaCl_2$, and 10 MES/Tris, pH 5.5). Transporter currents were evoked with Solution B

containing 20 mM sucrose. Solutions containing in addition 1 mM GSSG were freshly prepared at the day of each experiment.

Accession Numbers

Sequence data from this article can be found in the GenBank/EMBL data libraries under the following accession numbers: SUT1 from *S. tuberosum* (X69165), SUT1 from *S. lycopersicum* (X82275), and SUT1 from *Z. mays* (AB008464).

Supplemental Data

The following materials are available in the online version of this article.

Supplemental Figure 1. Methyl-β-Cyclodextrin Induced Cholesterol Depletion Can Destroy Raft-Like Structures, and *o*-Phtalaldehyde Cross-Linking Can Induce Raft-Like Structures when Sl SUT1-GFP Is Expressed in the Yeast Strain SUSY7.

Supplemental Figure 2. Calibration of the Molecular Mass of the SUT1 Monomer and Dimer in Blue Native Gels with the Molecular Mass of Known Soluble Marker Proteins.

ACKNOWLEDGMENTS

We thank Thomas Buckhout and Gernot Renger for support and helpful discussions as well as Claudia Oecking, Katrin Czempinsky, and Doris Rentsch for providing material. We thank Ulf Dühring for help with the cross-linking experiments, Aleksandra Hackel for excellent technical assistance, and Angelika Pötter for the care of greenhouse plants. This work was supported by the German Research Foundation DFG (SFB 429), Cluster of Excellence "Unifying Concepts in Catalysis," and the EU E-MeP program (B.P.) and a NWO *Veni* grant (to L.M.V.). Thanks to the anonymous reviewers for their helpful comments.

Received January 28, 2008; revised August 25, 2008; accepted September 3, 2008; published September 12, 2008.

REFERENCES

Alberini, C.M., Bet, P., Milstein, C., and Sitia, R. (1990). Secretion of immunoglobulin M assembly intermediates in the presence of reducing agents. Nature **347:** 485–487.

Alosi, M.C., Melroy, D.L., and Park, R.B. (1988). The regulation of gelation of phloem exudate from Cucurbita fruit by dilution, glutathione, and glutathione reductase. Plant Physiol. **86:** 1089–1094.

Andrews, L.B., and Curtis, W.R. (2005). Comparison of transient protein expression in tobacco leaves and plant suspension culture. Biotechnol. Prog. **21:** 946–952.

Balmer, Y., Vensel, W.H., Cai, N., Manieri, W., Schurmann, P., Hurkman, W.J., and Buchanan, B.B. (2006). A complete ferredoxin/thioredoxin system regulates fundamental processes in amyloplasts. Proc. Natl. Acad. Sci. USA **103:** 2988–2993.

Bjerrum, O.J., and Heegaard, N.H.H. (1988). Handbook of Immunoblotting of Proteins. (Boca Raton, FL: CRS Press).

Bolwell, P.P., Page, A., Pislewska, M., and Wojtaszek, P. (2001). Pathogenic infection and the oxidative defences in plant apoplast. Protoplasma **217:** 20–32.

Boorer, K.J., Loo, D.D., Frommer, W.B., and Wright, E.M. (1996). Transport mechanism of the cloned potato H^+/sucrose cotransporter StSUT1. J. Biol. Chem. **271:** 25139–25144.

Borner, G.H., Sherrier, D.J., Weimar, T., Michaelson, L.V., Hawkins, N.D., Macaskill, A., Napier, J.A., Beale, M.H., Lilley, K.S., and Dupree, P. (2005). Analysis of detergent-resistant membranes in Arabidopsis. Evidence for plasma membrane lipid rafts. Plant Physiol. **137:** 104–116.

Bourquin, S., Bonnemain, J.L., and Delrot, S. (1990). Inhibition of loading of C assimilates by p-chloromercuribenzenesulfonic acid: Localization of the apoplastic pathway in *Vicia faba.* Plant Physiol. **92:** 97–102.

Brown, D.A., and London, E. (1998). Functions of lipid rafts in biological membranes. Annu. Rev. Cell Dev. Biol. **14:** 111–136.

Bush, D.R. (1989). Proton-coupled sucrose transport in plasmalemma vesicles isolated from sugar beet (*Beta vulgaris* L. cv Great Western) leaves. Plant Physiol. **89:** 1318–1323.

Bush, D.R. (1993). Inhibitors of the proton-sucrose symport. Arch. Biochem. Biophys. **307:** 355–360.

Carpaneto, A., Geiger, D., Bamberg, E., Sauer, N., Fromm, J., and Hedrich, R. (2005). Phloem-localized, proton-coupled sucrose carrier ZmSUT1 mediates sucrose efflux under the control of the sucrose gradient and the proton motive force. J. Biol. Chem. **280:** 21437–21443.

Chincinska, I.A., Liesche, J., Krugel, U., Michalska, J., Geigenberger, P., Grimm, B., and Kuhn, C. (2008). Sucrose transporter StSUT4 from potato affects flowering, tuberization, and shade avoidance response. Plant Physiol. **146:** 515–528.

Diaz-Vivancos, P., Rubio, M., Mesonero, V., Periago, P.M., Barcelo, A.R., Martinez-Gomez, P., and Hernandez, J.A. (2006). The apoplastic antioxidant system in Prunus: Response to long-term plum pox virus infection. J. Exp. Bot. **57:** 3813–3824.

Flury, T., Wagner, E., and Kreuz, K. (1996). An inducible glutathione S-transferase in soybean hypocotyl is localized in the apoplast. Plant Physiol. **112:** 1185–1190.

Fra, A.M., Fagioli, C., Finazzi, D., Sitia, R., and Alberini, C.M. (1993). Quality control of ER synthesized proteins: An exposed thiol group as a three-way switch mediating assembly, retention and degradation. EMBO J. **12:** 4755–4761.

Franceschi, V.R., and Tarlyn, N.M. (2002). L-Ascorbic acid is accumulated in source leaf phloem and transported to sink tissues in plants. Plant Physiol. **130:** 649–656.

Gao, X.D., and Dean, N. (2000). Distinct protein domains of the yeast Golgi GDP-mannose transporter mediate oligomer assembly and export from the endoplasmic reticulum. J. Biol. Chem. **275:** 17718–17727.

Grossmann, G., Opekarova, M., Malinsky, J., Weig-Meckl, I., and Tanner, W. (2007). Membrane potential governs lateral segregation of plasma membrane proteins and lipids in yeast. EMBO J. **26:** 1–8.

Grossmann, G., Opekarova, M., Novakova, L., Stolz, J., and Tanner, W. (2006). Lipid raft-based membrane compartmentation of a plant transport protein expressed in *Saccharosmyces cerevisiae.* Eukaryot. Cell **5:** 945–953.

Gutscher, M., Pauleau, A.L., Marty, L., Brach, T., Wabnitz, G.H., Samstag, Y., Meyer, A.J., and Dick, T.P. (2008). Real-time imaging of the intracellular glutathione redox potential. Nat. Methods **5:** 553–559.

Hackel, A., Schauer, N., Carrari, F., Fernie, A.R., Grimm, B., and Kühn, C. (2006). Sucrose transporter LeSUT1 and LeSUT2 inhibition affects tomato fruit development in different ways. Plant J. **45:** 180–192.

Hanzal-Bayer, M.F., and Hancock, J.F. (2007). Lipid rafts and membrane traffic. FEBS Lett. **581:** 2098–2104.

He, H., Chincinska, I., Hackel, A., Grimm, B., and Kühn, C. (2008). Phloem mobility and stability of sucrose transporter transcripts. The Open Plant Science Journal **2:** 15–26.

Hendriks, J.H., Kolbe, A., Gibon, Y., Stitt, M., and Geigenberger, P. (2003). ADP-glucose pyrophosphorylase is activated by posttranslational redox-modification in response to light and to sugars in leaves of Arabidopsis and other plant species. Plant Physiol. **133:** 838–849.

Henriksen, U., Fog, J.U., Litman, T., and Gether, U. (2005). Identification of intra- and intermolecular disulfide bridges in the multidrug resistance transporter ABCG2. J. Biol. Chem. **280:** 36926–36934.

Heuberger, E.H., Veenhoff, L.M., Duurkens, R.H., Friesen, R.H., and Poolman, B. (2002). Oligomeric state of membrane transport proteins analyzed with blue native electrophoresis and analytical ultracentrifugation. J. Mol. Biol. **317:** 591–600.

Hu, X., Jiang, M., Zhang, A., and Lu, J. (2005). Abscisic acid-induced apoplastic H2O2 accumulation up-regulates the activities of chloroplastic and cytosolic antioxidant enzymes in maize leaves. Planta **223:** 57–68.

Ikonen, E. (2001). Roles of lipid rafts in membrane transport. Curr. Opin. Cell Biol. **13:** 470–477.

Ishiwatari, Y., Honda, C., Kawashima, I., Nakamura, S., Hirano, H., Mori, S., Fujiwara, T., Hayashi, H., and Chino, M. (1995). Thioredoxin h is one of the major proteins in rice phloem sap. Planta **195:** 456–463.

Jamai, A., Tommasini, R., Martinoia, E., and Delrot, S. (1996). Characterization of glutathione uptake in broad bean leaf protoplasts. Plant Physiol. **111:** 1145–1152.

Khan, Y.M., Starling, A.P., East, J.M., and Lee, A.G. (1996). The mechanism of inhibition of the Ca(2+)-ATPase of skeletal-muscle sarcoplasmic reticulum by the cross-linker o-phthalaldehyde. Biochem. J. **317:** 439–445.

Kolbe, A., Oliver, S.N., Fernie, A.R., Stitt, M., van Dongen, J.T., and Geigenberger, P. (2006). Combined transcript and metabolite profiling of Arabidopsis leaves reveals fundamental effects of the thiol-disulfide status on plant metabolism. Plant Physiol. **141:** 412–422.

Kühn, C. (2003). Comparison of the sucrose transporter systems of different plant species. Plant Biol. **5:** 215–232.

Kühn, C., Franceschi, V.R., Schulz, A., Lemoine, R., and Frommer, W.B. (1997). Macromolecular trafficking indicated by localization and turnover of sucrose transporters in enucleate sieve elements. Science **275:** 1298–1300.

Kühn, C., Quick, W.P., Schulz, A., Riesmeier, J., Sonnewald, U., and Frommer, W.B. (1996). Companion cell-specific inhibition of the potato sucrose transporter SUT1. Plant Cell Environ. **19:** 1115–1123.

Laemmli, U.K. (1970). Cleavage of structural proteins during the assembly of the head of bacteriophage T4. Nature **227:** 680–685.

Lajoie, P., and Nabi, I.R. (2007). Regulation of raft-dependent endocytosis. J. Cell. Mol. Med. **11:** 644–653.

Lalonde, S., Weise, A., Walsh, R.P., Ward, J.M., and Frommer, W.B. (2003). Fusion to GFP blocks intercellular trafficking of the sucrose transporter SUT1 leading to accumulation in companion cells. BMC Plant Biol. **3:** 8.

Larsson, C. (1985). Plasma Membranes. (Berlin: Springer-Verlag).

Laude, A.J., and Prior, I.A. (2004). Plasma membrane microdomains: organization, function and trafficking. Mol. Membr. Biol. **21:** 193–205.

Laughery, M.D., Todd, M.L., and Kaplan, J.H. (2003). Mutational analysis of alpha-beta subunit interactions in the delivery of Na, K-ATPase heterodimers to the plasma membrane. J. Biol. Chem. **278:** 34794–34803.

Lefebvre, B., Furt, F., Hartmann, M.A., Michaelson, L.V., Carde, J.P., Sargueil-Boiron, F., Rossignol, M., Napier, J.A., Cullimore, J., Bessoule, J.J., and Mongrand, S. (2007). Characterization of lipid rafts from *Medicago truncatula* root plasma membranes: A proteomic study reveals the presence of a raft-associated redox system. Plant Physiol. **144:** 402–418.

Lemaire, S.D., Miginiac-Maslow, M., and Jacquot, J.P. (2002). Plant thioredoxin gene expression: Control by light, circadian clock, and heavy metals. Methods Enzymol. **347:** 412–421.

Lemaire, S.D., Stein, M., Issakidis-Bourguet, E., Keryer, E., Benoit, V.V., Pineau, B., Gerard-Hirne, C., Miginiac-Maslow, M., and Jacquot, J.P. (1999). The complex regulation of ferredoxin/thioredoxin-related genes by light and the circadian clock. Planta **209:** 221–229.

Lemoine, R., Kühn, C., Thiele, N., Delrot, S., and Frommer, W.B. (1996). Antisense inhibition of the sucrose transporter: effects on amount of carrier and sucrose transport activity. Plant Cell Environ. **19:** 1124–1131.

Liang, Z., Veeraprame, H., Bayan, N., and Li, G. (2004). The C-terminus of prenylin is important in forming a dimer conformation necessary for endoplasmic-reticulum-to-Golgi transport. Biochem. J. **380:** 43–49.

Lichtner, F.T., and Spanswick, R.M. (1981). Sucrose uptake by developing soybean cotyledons. Plant Physiol. **68:** 693–698.

Liman, E., Tytgat, J., and Hess, P. (1992). Subunit stoichiometry of a mammalian K^+ channel determined by construction of multimeric cDNAs. Neuron **9:** 861–871.

Malinska, K., Malinsky, J., Opekarova, M., and Tanner, W. (2003). Visualization of protein compartmentation within the plasma membrane of living yeast cells. Mol. Biol. Cell **14:** 4427–4436.

Marino, D., Hohnjec, N., Küster, H., Moran, J., González, E., and Arrese-Igor, C. (2008). Evidence for transcriptional and post-translational regulation of sucrose synthase in pea nodules by the cellular redox state. Mol. Plant Microbe Interact. **21:** 622–630.

Maurel, C. (2007). Plant aquaporins: Novel functions and regulation properties. FEBS Lett. **581:** 2227–2236.

Maurousset, L., Lemoine, R., Gallet, O., Delrot, S., and Bonnemain, J.L. (1992). Sulfur dioxide inhibits the sucrose carrier of the plant plasma membrane. Biochim. Biophys. Acta **1105:** 230–236.

M'Batchi, B., and Delrot, S. (1984). Parachloromercuribenzenesulfonic acid: A potential tool for differential labeling of the sucrose transporter. Plant Physiol. **75:** 154–160.

Mesecke, N., Terziyska, N., Kozany, C., Baumann, F., Neupert, W., Hell, K., and Herrmann, J.M. (2005). A disulfide relay system in the intermembrane space of mitochondria that mediates protein import. Cell **121:** 1059–1069.

Mikosch, M., Hurst, A.C., Hertel, B., and Homann, U. (2006). Diacidic motif is required for efficient transport of the K^+ channel KAT1 to the plasma membrane. Plant Physiol. **142:** 923–930.

Mongrand, S., Morel, J., Laroche, J., Claverol, S., Carde, J.P., Hartmann, M.A., Bonneu, M., Simon-Plas, F., Lessire, R., and Bessoule, J.J. (2004). Lipid rafts in higher plant cells: purification and characterization of Triton X-100-insoluble microdomains from tobacco plasma membrane. J. Biol. Chem. **279:** 36277–36286.

Morel, J., Claverol, S., Mongrand, S., Furt, F., Fromentin, J., Bessoule, J.J., Blein, J.P., and Simon-Plas, F. (2006). Proteomics of plant detergent-resistant membranes. Mol. Cell. Proteomics **5:** 1396–1411.

Murphy, A.S., Bandyopadhyay, A., Holstein, S.E., and Peer, W.A. (2005). Endocytotic cycling of PM proteins. Annu. Rev. Plant Biol. **56:** 221–251.

Or, E., Goldshleger, R., Shainskaya, A., and Karlish, S.J. (1998). Specific cross-links between fragments of proteolyzed Na,K-ATPase induced by o-phthalaldehyde. Biochemistry **37:** 8197–8207.

Palmgren, M.G. (1990). An H-ATPase assay: Proton pumping and ATPase activity determined simultaneously in the same sample. Plant Physiol. **94:** 882–886.

Palmgren, M.G., and Sommarin, M. (1989). Lysophosphatidylcholine stimulates ATP dependent proton accumulation in isolated oat root plasma membrane vesicles. Plant Physiol. **90:** 1009–1014.

Parton, R.G., and Richards, A.A. (2003). Lipid rafts and caveolae as portals for endocytosis: New insights and common mechanisms. Traffic **4:** 724–738.

Reinders, A., Schulze, W., Kühn, C., Barker, L., Schulz, A., Ward, J. M., and Frommer, W.B. (2002). Protein-protein interactions between sucrose transporters of different affinities colocalized in the same enucleate sieve element. Plant Cell **14:** 1567–1577.

Riesmeier, J.W., Hirner, B., and Frommer, W.B. (1993). Potato sucrose transporter expression in minor veins indicates a role in phloem loading. Plant Cell **5:** 1591–1598.

Riesmeier, J.W., Willmitzer, L., and Frommer, W.B. (1992). Isolation and characterization of a sucrose carrier cDNA from spinach by functional expression in yeast. EMBO J. **11:** 4705–4713.

Riesmeier, J.W., Willmitzer, L., and Frommer, W.B. (1994). Evidence for an essential role of the sucrose transporter in phloem loading and assimilate partitioning. EMBO J. **13:** 1–7.

Roblin, G., Sakr, S., Bonmort, J., and Delrot, S. (1998). Regulation of a plant plasma membrane sucrose transporter by phosphorylation. FEBS Lett. **424:** 165–168.

Salahpour, A., Angers, S., Mercier, J.F., Lagace, M., Marullo, S., and Bouvier, M. (2004). Homodimerization of the beta2-adrenergic receptor as a prerequisite for cell surface targeting. J. Biol. Chem. **279:** 33390–33397.

Samaj, J., Baluska, F., Voigt, B., Schlicht, M., Volkmann, D., and Menzel, D. (2004). Endocytosis, actin cytoskeleton, and signaling. Plant Physiol. **135:** 1150–1161.

Schägger, H., Cramer, W.A., and von Jagow, G. (1994). Analysis of molecular masses and oligomeric states of protein complexes by blue native electrophoresis and isolation of membrane protein complexes by two-dimensional native electrophoresis. Anal. Biochem. **217:** 220–230.

Simons, K., and Ikonen, E. (1997). Functional rafts in cell membranes. Nature **387:** 569–572.

Szederkényi, J., Komor, E., and Schobert, C. (1997). Cloning of the cDNA for glutaredoxin, an abundant sieve-tube exudate protein from *Ricinus communis* L. and characterisation of the glutathione-dependent thiol-reduction system in sieve tubes. Planta **202:** 349–356.

Thompson, M.V., and Wolniak, S.M. (2008). A plasma membrane-anchored fluorescent protein fusion illuminates sieve element plasma membranes in Arabidopsis and tobacco. Plant Physiol. **146:** 1599–1610.

Vanacker, H., Carver, T.L., and Foyer, C.H. (1998). Pathogen-induced changes in the antioxidant status of the apoplast in barley leaves. Plant Physiol. **117:** 1103–1114.

Veenhoff, L.M., Heuberger, E.H., and Poolman, B. (2002). Quaternary structure and function of transport proteins. Trends Biochem. Sci. **27:** 242–249.

Walter, M., Chaban, C., Schutze, K., Batistic, O., Weckermann, K., Nake, C., Blazevic, D., Grefen, C., Schumacher, K., Oecking, C., Harter, K., and Kudla, J. (2004). Visualization of protein interactions in living plant cells using bimolecular fluorescence complementation. Plant J. **40:** 428–438.

Walz, C., Juenger, M., Schad, M., and Kehr, J. (2002). Evidence for the presence and activity of a complete antioxidant defence system in mature sieve tubes. Plant J. **31:** 189–197.

Wang, Q., Monroe, J., and Sjolund, R.D. (1995). Identification and characterization of a phloem-specific beta-amylase. Plant Physiol. **109:** 743–750.

Weise, A., Barker, L., Kühn, C., Lalonde, S., Buschmann, H., Frommer, W.B., and Ward, J.M. (2000). A new subfamily of sucrose transporters, SUT4, with low affinity/high capacity localized in enucleate sieve elements of plants. Plant Cell **12:** 1345–1355.

Weise, A., Lalonde, S., Kühn, C., Frommer, W.B., and Ward, J.M. (2008). Introns control expression of sucrose transporter LeSUT1 in trichomes, companion cells and in guard cells. Plant Mol. Biol. **68:** 251–262.